Simulation calculation of the ion-dynamic effect on overlapping neutral helium lines

A. Calisti, R. Stamm, and B. Talin
Physique des Interactions Ioniques et Moléculaires, Université de Provence, Centre de St. Jérôme, F-13397 Marseille Cédex 13, France
(Received 16 May 1988)

Using a computer-simulation model, we have investigated ion dynamic effects on the spectral line shape of the neutral helium line 4471 Å. For electron densities of arc plasma conditions (10^{15} cm$^{-3} \leq n_e \leq 10^{16}$ cm^{-3}), our simulation profiles are compared with experimental profiles. We discuss our results in comparison with calculations based on the static ion approximation, and with results including ion-dynamic effects treated by the model microfield method or a generalized collision operator approach.

The last two decades have seen continuous experimental and theoretical activity to study ion dynamic effects in the Stark broadening of helium lines. Indeed, as early as 1970, Burgess[1] suggested that by taking consideration of the line-broadening formalisms of the relative motion between the emitter and the ion perturber, one could explain the theory-experiment discrepancies of the He *I* $2\,^3P$–$4\,^3D$ line at 4471 Å, and its nearby 2^3P-4^3F forbidden component. For this atomic system, several theoretical models taking account of the ion-dynamic effect have been proposed that improve the agreement with the measured profiles. Among those are approaches based on a generalized collisional damping operator,[2–4] but also the so-called Model Microfield Method[5] (MMM), which uses static and dynamic properties of the plasma microfield. While the overall shape of the 4471-Å line is generally well predicted by these approaches, there remain differences with recent accurate experimental profiles,[6,7] especially in the position and intensity of the forbidden component, leaving desirable a new and independent calculation. In this paper we report about the use of a simulation calculation for the ionic component of the plasma, and discuss the resulting line profile in comparison with experiments and other calculations.

The simulation technique described below has already been used to study ion-dynamic effects on the line shape of the Lyman and Balmer series[8,9] of hydrogen emitters in arc plasma conditions. The result of these simulation studies is that the ion-dynamic effect is responsible for almost all of the difference between a theory with static ions and the experimental profiles. We have used here a similar simulation technique for the ionic component of the plasma interacting with a neutral helium emitter. The line shape is expressed as a Fourier transform of the emitters dipole autocorrelation function:

$$I(\omega)=\mathrm{Re}\left[(1/\pi)\int_0^{+\infty}\exp[i(\omega+\omega_0)t]C(t)dt\right], \qquad (1)$$

where ω_0 is the unperturbed frequency of the transition, and $C(t)$ is the emitters dipole autocorrelation function:

$$C(t)=\langle \mathbf{d}(t)\cdot\mathbf{d}(0)\rangle . \qquad (2)$$

In this expression, $\mathbf{d}$ is the emitters dipole operator, and the bracket denotes an average over the emitters internal degrees of freedom, the electronic screened ionic component, and the electronic component of the plasma. This electronic component will be treated by an impact operator,[10] which should be accurate enough in the central region of the line where ion-dynamic effects are expected.

For the ionic component, we have used a computer simulation-technique that has already been applied to the calculation of hydrogen lines.[8,9] In this simulation model, we calculate the electric field due to N ions (with usually $N=125$ ions), at the center of a sphere of radius R using the following expression:

$$\boldsymbol{\epsilon}=\sum_j \boldsymbol{\epsilon}_j=\sum_j (e\mathbf{r}_j/r_j^3)(1+r_j/\lambda_D)\exp(-r_j/\lambda_D), \qquad (3)$$

where $\mathbf{r}_j$ is the position of the jth ion, $\lambda_D=(kT/4\pi n_e e^2)^{1/2}$ is the Debye length, n_e being the electron density. Velocities are given to the ions according to a Maxwell law corresponding to the reduced mass of the helium emitter, ion perturber pair. With our quasiparticle model, each ion moves on a straight line in the sphere. If a particle j exists the sphere between two times t_i and t_{i+1}, it is replaced by a new particle located at a point $r_{j,\mathrm{new}}$ chosen at random in the spherical shell defined by $r_j(t_i)\leq r_{j,\mathrm{new}}\leq R$. The new velocity is taken equal to $\mathbf{v}_j$ or replaced by $-\mathbf{v}_j$ if $\mathbf{v}_j\cdot\mathbf{r}_{j,\mathrm{new}}$ is positive. One configuration of the ionic field is generated by following the particles over a time equal to a few times $\omega_{\mathrm{pi}}^{-1}$, where ω_{pi} is the ion plasma frequency. The dipole autocorrelation function is then obtained by averaging the following expression over a subset of microfield configurations:

$$\langle \mathbf{d}(t)\cdot\mathbf{d}(0)\rangle=\sum_{\alpha',\alpha'',\beta}\mathbf{d}_{\alpha'\beta}\cdot\mathbf{d}_{\alpha''\beta}\langle T_{\alpha'\alpha''}\rangle , \qquad (4)$$

where the sum is over the upper levels α',α'' of the transition, β denotes the lower level of the transition that is assumed to be unperturbed, and T is the time evolution operator of the emitter. We have calculated this dipole

autocorrelation function for electronic densities 10^{15} cm$^{-3} \leq n_e \leq 10^{16}$ cm^{-3}, a density domain where several accurate measurements of the 4471-Å line are available. In this density range, we can ignore the influence of the lower 2^3S level, and of the upper 4^3P level, because of their large energy separation with, respectively, the lower 2^3P level and upper 4^3D, 4^3F levels. In addition we can neglect for $n_e \geq 10^{15}$ cm^{-3} the fine structure of the triplet levels. Using the spherical quantum numbers we denote the lower state as $|\beta\rangle = |21m_\beta\rangle$, and the upper states as $|\alpha\rangle = |4,l_\alpha,m_\alpha\rangle$, with l_α equal to 2 or 3.

The emitters evolution operator obeys the following Schrödinger equation:

$$i\hbar\frac{\partial T}{\partial t} = (H_0 + \Phi_e - \mathbf{d}\cdot\boldsymbol{\epsilon})T \ , \tag{5}$$

where H_0 is the unperturbed Hamiltonian, $\boldsymbol{\epsilon}$ is the ionic microfield, and Φ_e is the electronic collision operator. This operator is diagonal in the spherical quantum number basis and is well approximated by the so-called high-temperature limit,[10] which is written omitting the negligible shift[11]

$$(\Phi_e)_{ll} = -3(2\pi m_e/kT)^{1/2}(\hbar/m_e)^2 n_e[n^2/(2l+1)] \times\{(l+1)[n^2-(l+1)^2][\tfrac{1}{2}+\ln(2kT/n^2\hbar\omega_{l,l+1})]+l(n^2-l^2)[1/2+\ln(2kT/n^2\hbar\omega_{l,l-1})]\} \ , \tag{6}$$

where the frequencies $\omega_{l,l\pm1}$ are defined as

$$\omega_{l,l\pm1} = \max[\,|\omega_l - \omega_{l\pm1}|\,, \omega_p = (4\pi n_e e^2/m_e)^{1/2}] \ , \tag{7}$$

ω_p being the electronic plasma frequency and ω_l the frequency of level l.

The Schrödinger equation for T is numerically solved for each configuration by using a fast differential equation solver. Accurate line profiles are obtained with only a few hundred configurations when noise-filtering techniques are used as described in Ref. 8. Some statistical noise remains and is observed on the line profiles, but we have found that the central part of the line was each time reproduced to better than 5%, when different subsets of 220 configurations were used.

In order to demonstrate the effect of ion dynamics on the dipole autocorrelation function, we have plotted on Fig. 1 this function $C(t)$ for static and dynamic ions. A criterion for ignoring the role of ion dynamics is that the correlation time of the emitters dipole correlation function taken in the static ion approximation (dashed-line curve) is much smaller than the inverse of the ion plasma frequency.[8] This is not the case for the plasma conditions of Fig. 1, and never is the case for the density range that we have considered. The solid-line curve on Fig. 1 is the dipole correlation function taking account of ion dynamics. Compared to the dipole correlation function in the static ion approximation, it demonstrates the additional damping effect due to ion dynamics.

Our first simulation calculations have been made for densities $n_e = 10^{15}$ cm^{-3} and $n_e = 3\times10^{15}$ cm^{-3}, and electronic and ionic temperatures T_e and T_0 corresponding to the experiment of Piel and Richter in 1983.[6] These experimental profiles are plotted in Figs. 2 and 3, as well as the simulation results in the static and dynamic ion case. The simulation profiles are convolved with a Doppler profile, and also with an instrumental profile whose width

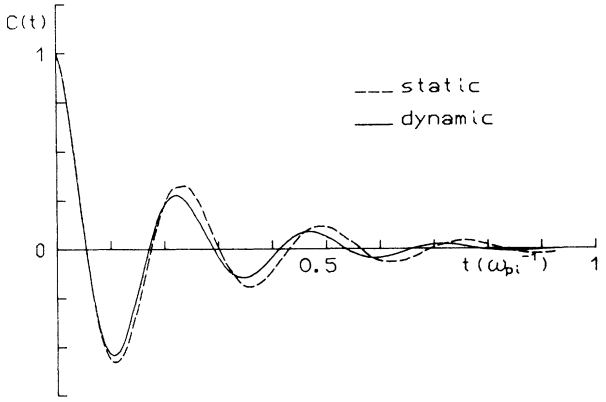

FIG. 1. Dipole autocorrelation function of the He I 4471-Å line for a simulation with static ions (dashed line) and dynamic ions (solid line), at $n_e = 10^{15}$ cm^{-3}, ionic temperature $T_0 = 15\,000$ K, and electronic temperature $T_e = 20\,000$ K.

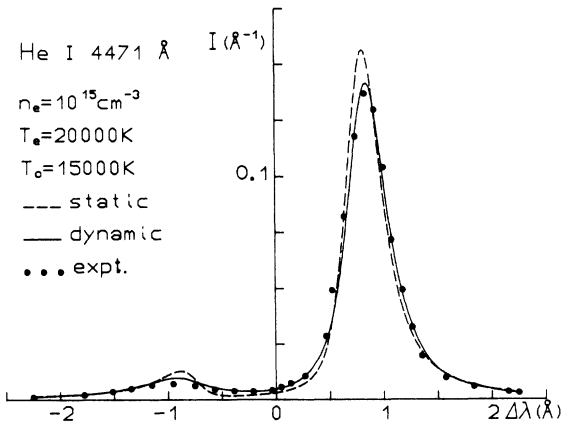

FIG. 2. Comparison of static ions (dashed line), dynamic ions (solid line), and experimental (Ref. 6) (dots) He I 4471-Å line profiles for a density $n_e = 10^{15}$ cm^{-3}, ionic temperature $T_0 = 15\,000$ K, and electronic temperature $T_e = 20\,000$ K.

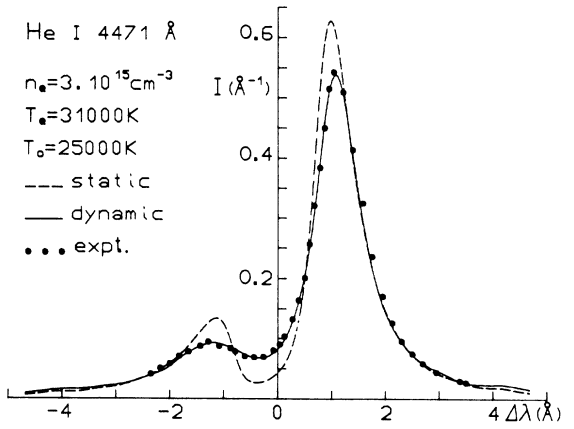

FIG. 3. Same as Fig. 2 for $n_e=3\times10^{15}$ cm^{-3}, $T_0=25\,000$ K, and $T_e=31\,000$ K.

is 6×10^{-10} cm.[6] Another simulation at $n_e=10^{16}$ cm^{-3} has been compared to an earlier experiment[12] in Fig. 4. As already well known, the profiles calculated by using the static ion approximation predict a central structure of the line which is completely different from what is seen in the experimental profiles. On the other hand, we observe a remarkable agreement between the simulation and the experimental profiles for all the three densities considered. We have compared these results with other theoretical profiles based on MMM calculations,[5] and on calculations using the generalized collision operator approach of Ref. 3 [Barnard, Cooper, and Smith (BCS)]. For the lowest density considered, the weak intensity of the forbidden peak calculated by the simulation is in agreement with BCS, but compared to the experiment

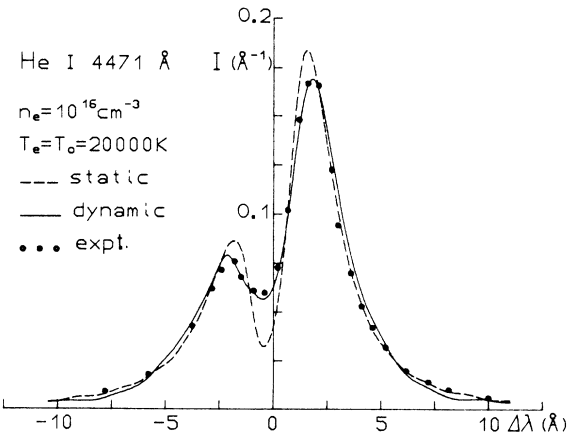

FIG. 4. Comparison of static ions (dashed line), dynamic ions (solid line), and experimental (Ref. 12) (dots) He I 4471-Å line profiles for a density $n_e=10^{16}$ cm^{-3}, and temperature $T_0=T_e=20\,000$ K.

these two approaches are 30% higher, while MMM is 45% higher. The peak separation, in agreement between the simulation, BCS, and the experiment, is smaller by about 10% on the MMM profile. On the other hand, the only significant deviation from the allowed component of the experimental profile is found in the BCS profile whose width is slightly too large.[6] For the two higher densities, the whole simulation profile is in good agreement with the experiment, while the maximum intensity of the forbidden component is 15% higher for BCS or MMM. Finally, for the conditions of Figs. 3 and 4 the peak separation is too small for MMM by about 10%, and the width of the allowed component is too large in the BCS calculations (by about 15% for $n_e=3\times10^{15}$ cm^{-3}).

Another way of investigating the effect of ion dynamics has been the study of profiles corresponding to different reduced mass μ of the helium emitter, ion perturber pair.[13] For a density $n_e=10^{15}$ cm^{-3} we have calculated for different temperatures the line profiles corresponding to three different values of μ: $\mu=0.8$ for a He-H^+ plasma, $\mu=2$ for a He-He^+ plasma, and $\mu=3.6$ for a He-Ar^+ plasma. In Fig. 5 we have plotted the relative dip $D_r=\{(I_{\max})_f-I_{\min}\}/(I_{\max})_f$, where $(I_{\max})_f$ is the maximum intensity of the forbidden component and $I_{\min}$ is the central minimum, as a function of $(T/\mu)^{1/2}$, a quantity that is proportional to the relative emitter-perturber velocity. The three experimental points[6,7] compare well with the simulation values, in contradiction with calculations from other approaches like MMM or BCS, which are in significant disagreement for this quantity.[7]

In conclusion, we have applied a computer-simulation technique to study the effect of ion dynamics on the 4471-Å line of neutral helium in arc plasma conditions. Similarly to simulation calculations of Lyman[8] and Balmer[9] hydrogen lines, excellent agreements have been found with experimental profiles of the He I $2\,^3p$-$4\,^3D,4\,^3F$. As already observed in other calculations including ion-dynamic effects, the profiles obtained have less structure than profiles obtained by using the static

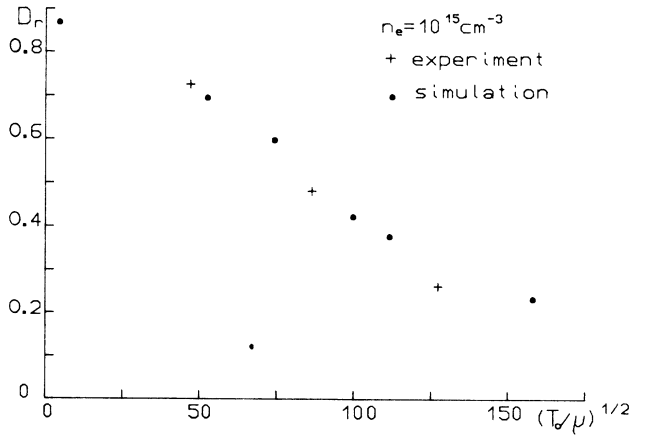

FIG. 5. Simulation (dots) and experimental (Refs. 6 and 7) (crosses) relative dip D_r as a function of $(T_0/\mu)^{1/2}$ at $n_e=10^{15}$ cm^{-3}.

ion approximation. A general tendency due to ion dynamics is the filling of the transition region between the allowed and forbidden component, and a reduction of the forbidden component intensity. The close quantitative agreement of the simulation with the experiment excludes for this line the presence of a significant unidentified broadening mechanism in the usual conditions of arc plasmas.

Équipe de Recherche No. 773 associée au Centre National de la Recherche Scientifique.

[1]D. D. Burgess, J. Phys. B **3**, L70 (1970).

[2]R. W. Lee, J. Phys. B **6**, 1044 (1973).

[3]A. J. Barnard, J. Cooper, and E. W. Smith, J. Quant. Spectrosc. Radiat. Transfer **14**, 1025 (1974).

[4]D. Voslamber and E. R. A. Segre, J. Quant. Spectrosc. Radiat. Transfer **25**, 45 (1981).

[5]A. Brissaud, C. Goldbach, J. Leorat, A. Mazure, and G. Nollez, J. Phys. B **9**, 1147 (1976).

[6]A. Piel and A. Richter, Z. Naturforsch. **38a**, 37 (1983).

[7]V. Helbig, in *Spectral Line Shape III,* edited by F. Rostas (De Gruyter, Berlin, 1985), p. 3.

[8]R. Stamm and E. W. Smith, Phys. Rev. A **30**, 450 (1984); R. Stamm, E. W. Smith, and B. Talin, *ibid.* **30**, 2039 (1984); R. Stamm, B. Talin, E. L. Pollock, and C. A. Iglesias, *ibid.* **34**, 4144 (1986).

[9]J. Seidel, in *Spectral Line Shape III,* edited by F. Rostas (De Gruyter, Berlin, 1985), p. 69.

[10]H. R. Griem, *Spectral Line Broadening by Plasmas* (Academic, New York, 1974).

[11]H. R. Griem, Astrophys. J. **154**, 1111 (1968).

[12]J. W. Birkeland, M. E. Bacon, and W. G. Braun, Phys. Rev. A **3**, 354 (1971).

[13]C. Fleurier, G. Coulaud, and J. Chapelle, Phys. Rev. A **18**, 575 (1978).